

Simultaneous photoluminescence import and mechanical enhancement of polymer films using silica-hybridized quantum dots†

Li Zhou,^{ab} Chao Gao^{*a} and Weijian Xu^{*b}

Received 29th January 2010, Accepted 15th April 2010

First published as an Advance Article on the web 7th June 2010

DOI: 10.1039/c0jm00211a

Quantum dot (QD)-polymer nanocomposites that simultaneously possess stable photoluminescence and enhanced mechanical properties are presented for the first time based on the facile blending of the ultrasmall silica-hybridized CdTe QDs (SiO₂-*h*-QDs) or 3-(trimethoxysilyl)propyl methacrylate-modified SiO₂-*h*-QDs (SiO₂-*h*-QD-MSMAs) with polymer. Typically, for SiO₂-*h*-QD-MSMA/poly(methyl methacrylate) (PMMA) nanocomposite films, the tensile strength, Young's modulus, and elongation at break improved by about 46%, 74% and 6%, respectively, upon the loading of only 0.2 wt% of SiO₂-*h*-QD-MSMAs. It is found that the mechanical enhancement effect of the silica-hybridized QDs is general for both hydrophilic polymers such as polyvinyl alcohol and hydrophobic polymers such as PMMA or polystyrene due to the strong interfacial adhesion between SiO₂-*h*-QDs and polymer matrix as well as the fine dispersibility of the nanofillers in composites. SEM measurements showed a ductile-rupture behavior for the materials in which the surface-modified nanofillers were well compatible with the polymer matrix, but a brittle-rupture behavior for the composites loaded with pristine nanofillers due to their local aggregation. The loading of silica-hybridized QDs simultaneously endowed the composites with desired and stable optical properties. No obvious decreases of both photoluminescence and transparency were found for the nanocomposite films exposed to daylight even for one year. Such dual functional SiO₂-*h*-QD-polymer nanocomposites promise great potential to upgrade the conventional polymer materials.

Introduction

Nanocomposites that consist of polymers and inorganic components are of interest owing to their enhanced mechanical, optical, and thermal properties as compared to the corresponding polymer or inorganic component only.^{1,2} Recently, fluorescent quantum dot (QD)-polymer nanocomposites have attracted considerable attention because of their wide potential applications in nonlinearly optical devices, optical displays, and solar cells.³⁻⁵ In this regard, numerous literatures have been published, however, they only focus on the photoluminescence properties of QDs.⁶⁻¹² Since most QDs have two intrinsic characteristics of photoluminescence and ultrasmall size, this situation leads to a big question that must be answered before the composites could be considered for true applications: how does the addition of ultrafine nanofillers of QDs influence the bulk property, especially mechanical properties, of the polymer matrix?

Unfortunately, to the best of our knowledge, no reports on the mechanical properties of the QDs-polymer can be found. Apparently, such a huge omission is not caused by the unimportance or the unattraction of this issue, but likely by the extreme difficulty in the large-scale fabrication of nanocomposites with both stable photoluminescence and good mechanical properties. It is known that the surface of QDs is susceptible to the external environment that can cause significant photoluminescence (PL) attenuation during the fabrication process of nanocomposites. Furthermore, the productivity of QDs that for biological applications such as bioimaging and biosensor would be adequate but for composites fabrication is too low considering the requirement of the dosage. Herein, we aim to resolve this challenge to open the avenue to multifunction and high performance QDs-polymer composites by employing highly stable and scalably produced silica-hybridized CdTe QDs (SiO₂-*h*-QDs) as the nanofillers.

Experimental

Materials

Tellurium powder (99.8%), CdCl₂ (99+%), NaBH₄ (96%), mercaptopropionic acid (MPA, 99+%), 1-thioglycerol (TG, 90+%), tetraethyl orthosilicate (TEOS, 98%), and 3-(trimethoxysilyl)propyl methacrylate (98%, MSMA) were purchased from Sigma-Aldrich and used as received. Silica with mean diameter 30 nm was purchased from Shandong Hina Co., Ltd (China). All other reagents are of analytical grades and used without further purification.

^aMOE Key Laboratory of Macromolecular Synthesis and Functionalization, Department of Polymer Science and Engineering, Zhejiang University, 38 Zheda Road, Hangzhou, 310027, P. R. China. E-mail: chaogao@zju.edu.cn

^bInstitute of Polymer Science and Engineering, College of Chemistry and Chemical Engineering, Hunan University, Changsha, 410082, P. R. China. E-mail: weijianxu@hnu.cn

† Electronic supplementary information (ESI) available: Emission spectra of SiO₂-*h*-QD-MSMA/PMMA films with different contents of SiO₂-*h*-QD-MSMAs, and representative stress-strain curves of pure PVA, SiO₂-*h*-QD/PVA nanocomposites, pure PS, and PS composites filled with unmodified SiO₂-*h*-QDs and SiO₂-MSMAs. See DOI: 10.1039/c0jm00211a

Synthesis of SiO₂-*h*-QDs and SiO₂-*h*-QD-MSMAs nanohybrids

Water-soluble silica-hybridized CdTe quantum dots (SiO₂-*h*-QDs) with average diameter 13 nm were prepared in aqueous solution by a one-pot approach.¹³ Typically, 20 mL of fresh NaHTe aqueous solution (2.2 M) was added to 10 L of N₂-saturated CdCl₂ solution (5.28 mM) at pH 9.0 adjusted by NaOH (1.0 M) in the presence of MPA (19.24 g, 178.2 mmol) at 100 °C. After 10 min, 360 mL of TEOS was added into the mixture. Then the mixture was refluxed for 24 h before the SiO₂-*h*-QDs nanohybrids were precipitated by ethanol. The supernatant was discarded, and the nanohybrids were centrifuged and washed with ethanol repeatedly. After purification, the resulting orange solid was dried at 60 °C for 24 h under vacuum, obtaining SiO₂-*h*-QDs nanohybrids (105.4 g, quantum yield: 11.7%, density: 2.5 g/cm³) with yellow luminescence under UV light (if TG is chosen as ligand instead of MPA, nanohybrids with green luminescence can be obtained).

For preparation of SiO₂-*h*-QD-MSMA, typically, 1.5 g of as prepared SiO₂-*h*-QDs nanohybrids were mixed with 50 mL of ethanol, and 1.2 mL of MSMA in a flask. The mixture was stirred for 12 h at room temperature. Diethyl ether was then added, and the precipitate was isolated by centrifugation. The resulting solids (SiO₂-*h*-QD-MSMA) show excellent dispersibility in organic solvents, such as chloroform (CHCl₃), N,N-dimethylformamide (DMF), *etc.* The SiO₂-MSMAs nanohybrids were prepared using the same procedure as for the SiO₂-*h*-QD-MSMAs but with the use of pure SiO₂.

Preparation of SiO₂-*h*-QD-polymer nanocomposite

For SiO₂-*h*-QD/PVA nanocomposite, it can be prepared by direct solution blending of polyvinyl alcohol (PVA) and SiO₂-*h*-QDs in aqueous solution. For SiO₂-*h*-QD-MSMA/PMMA or SiO₂-*h*-QD-MSMA/PS nanocomposites, they can also be facily prepared by solution blending of polymethylmethacrylate (PMMA) or polystyrene (PS) and SiO₂-*h*-QD-MSMA in CHCl₃. Then the intermixed solution of SiO₂-*h*-QD-MSMAs nanohybrids and polymer was cast into a petri dish, followed by solvent evaporation to obtain SiO₂-*h*-QD-MSMA/polymer nanocomposite. For comparison, PS composites filled with pristine SiO₂-*h*-QDs or SiO₂-MSMAs were also fabricated using the same procedure as for the case of SiO₂-*h*-QD-MSMAs.

Characterization

Thermal gravimetric analysis (TGA) was carried out on a PE TGA-7 instrument with a heating rate of 20 °C min⁻¹ in a nitrogen flow (20 mL min⁻¹). Fourier transform infrared (FTIR) spectra were recorded using a PE Paragon 1000 spectrometer (KBr disk). UV-vis spectra were recorded on a PE Lambda 20/2.0 UV/vis spectrometer. Emission spectra were collected using a Varian Cary 100 spectrometer. Transmission electron microscopy (TEM) studies were performed on a JEOL JEL2010 electron microscope at 200 kV. Scanning electron microscopy (SEM) images were recorded using a FEISIRION 200 field-emission microscope. The stress-strain curves of composites were measured using a RGWT mechanical tester (Shenzhen Reger Instrument Co., Ltd., China) at room

temperature. The strain rate was 20 mm min⁻¹. At least four measurements were performed for each composite.

Results and discussion

To design the QDs-polymer nanocomposites with desired integrated properties and application potentials, normally, the nanofillers of QDs would match the following requirements: (1) high stability of both structure and properties, (2) good dispersibility in the matrix, (3) small size to avoid sedimentation effects and phase separation. In short, a kind of ultrafine stable QDs with surface functional tailorability is needed. In addition, it should be prepared cost-effectively.

To obtain stable QDs, coatings of polymers and inorganic shells such as silica are generally employed to avoid the direct contact between QDs and surroundings.¹⁴⁻¹⁹ However, large-scale preparation of such core-shell nanomaterials with a cost-effective manner is yet to be explored. Most recently, we developed a one-pot strategy for scalable fabrication of silica-hybridized CdTe QDs (SiO₂-*h*-QDs) in aqueous solution.¹³ The structure of the SiO₂-*h*-QDs is not an exact core-shell structure (QD@SiO₂) with solely single QD in the middle of silica as previously reported,^{20,21} but in the form of a hybrid in which QDs are embedded in silica. The ultrafine SiO₂-*h*-QDs (<20 nm) can be facily obtained on a subkilogram-scale in one batch, and have been demonstrated to be highly stable in buffer solution and even cells as well as during chemical reactions, arousing the interest of the industrial application of QDs.¹³ Hence, we select this kind of SiO₂-*h*-QDs as the key raw material for fabrication of QDs-polymer composites.

Owing to the silica hybridization, the surface of the SiO₂-*h*-QDs can be easily tailored by silane-coupling chemistry. This is very important for preparing different kinds of SiO₂-*h*-QD-polymer nanocomposites because for hydrophilic polymers such as polyvinyl alcohol (PVA) the as-prepared water-soluble SiO₂-*h*-QDs can be directly utilized, but for hydrophobic polymers such as PMMA and PS, the SiO₂-*h*-QDs surfaces should be tailored with nonpolar molecules before blending with the polymers. Herein, we chose 3-(trimethoxysilyl)propyl methacrylate (MSMA) to modify the SiO₂-*h*-QDs surfaces and the reaction was monitored by thermal gravimetric analysis (TGA) and Fourier transform infrared (FTIR) spectra, as shown in Fig. 1a, b. For the crude SiO₂-*h*-QDs, only *ca.* 2% weight loss was found below 600 °C, while after the surface modification, the weight loss increased to *ca.* 11.3 wt% between 100–500 °C. In addition, from the FTIR spectra, after the modification, the carbonyl absorption band at 1725 cm⁻¹, and two obvious bands at 2856 and 2936 cm⁻¹ associated with C-H stretching appeared. All these demonstrated the successful formation of MSMA-immobilized SiO₂-*h*-QDs (SiO₂-*h*-QD-MSMA). It is worth noting that the crude SiO₂-*h*-QDs can only be dissolved in water and would be precipitated immediately in organic solvents while the SiO₂-*h*-QD-MSMAs showed good dispersibility in ethanol, tetrahydrofuran (THF), and even in chloroform, paving the way for the preparation of nanocomposites with hydrophobic polymers.¹³ More significantly, after the modification, the SiO₂-*h*-QD-MSMAs can still show excellent optical properties because of the silica interlayer protection (Fig. 1c). The small red-shift of SiO₂-*h*-QD-MSMAs in both absorption and emission may be

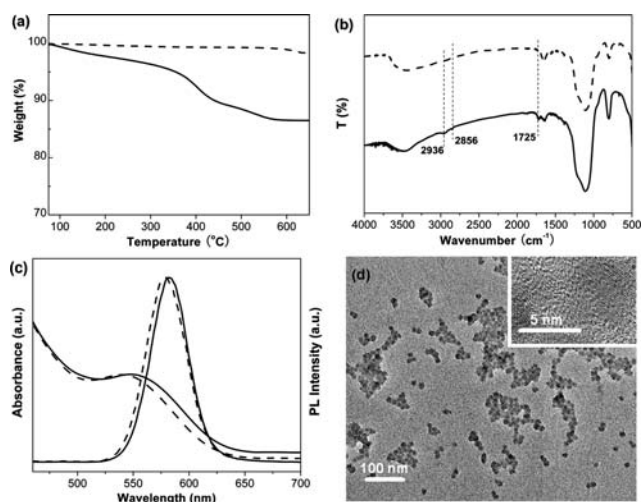


Fig. 1 TGA curves (a), FTIR spectra (b), absorption and photoluminescence (PL) spectra (c) of SiO₂-*h*-QD nanohybrids before (dashed line) and after (solid line) tailoring by MSMA (SiO₂-*h*-QD-MSMA). (d) TEM images of SiO₂-*h*-QD nanohybrids. The inset of (d) shows the high-resolution TEM image, confirming the existence of well-crystallized CdTe QDs.

caused by the solvent effect, since the SiO₂-*h*-QDs were measured in aqueous solution while SiO₂-*h*-QD-MSMAs in ethanol solution. In contrast, the photoluminescence of neat CdTe QDs would be quenched in 30 min during a common reaction such as esterification in our control experiments. In addition, we have demonstrated that the SiO₂-*h*-QDs showed much less toxicity than neat CdTe QDs, which is also quite important in the material use.¹³ Therefore, the SiO₂-*h*-QDs exceed neat QDs overwhelmingly in all aspects of stability, functional tailorability, environmental friendship, processability, productivity, and expense.

On the basis of their good solubility, through simple blending of the as-prepared SiO₂-*h*-QDs with PVA in aqueous solution, or SiO₂-*h*-QD-MSMAs with PMMA in chloroform solution, followed by solvent evaporation, wonderful nanocomposite films of SiO₂-*h*-QD/PVA or SiO₂-*h*-QD-MSMA/PMMA were obtained. The addition of SiO₂-*h*-QDs or SiO₂-*h*-QD-MSMAs can endow strong photoluminescence properties to polymer films without compromising the transparency as shown in Fig. 2a–c (also see ESI† Fig. S1). Compared with SiO₂-*h*-QDs, no obvious changes in the absorption and emission spectra of SiO₂-*h*-QD/PVA and SiO₂-*h*-QD-MSMA/PMMA films could be found, demonstrating that the structure and surface of the QDs were well retained during the process of film fabrication (Fig. 2a). Furthermore, compared with the corresponding neat polymer, the SiO₂-*h*-QD/PVA and SiO₂-*h*-QD-MSMA/PMMA films (the thickness is 0.7 mm) are also highly transparent and almost colourless even when the load content of SiO₂-*h*-QDs rose to 0.5 wt% as demonstrated by the UV-vis transmittance spectra (Fig. 2b). Films with different luminescence colours can be readily prepared by loading different SiO₂-*h*-QDs nanohybrids as shown in Fig. 2c. For example, SiO₂-*h*-QDs with yellow and green photoluminescence can be synthesized by using mercaptopropionic acid (MPA) and 1-thioglycerol (TG) as ligand, respectively. Significantly, the optical properties of the composite

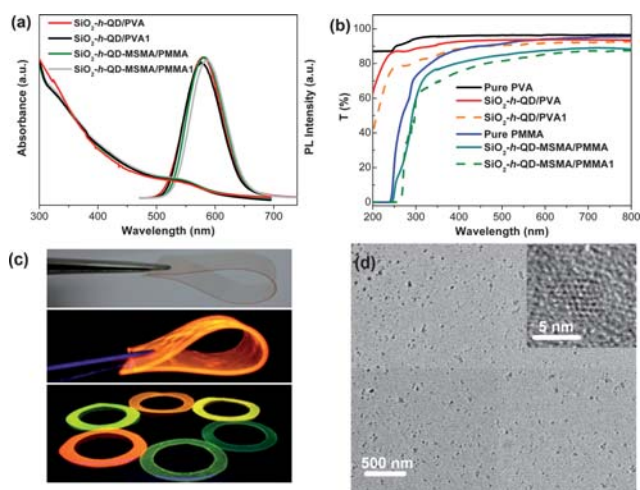


Fig. 2 (a) Absorption and emission spectra of newly prepared SiO₂-*h*-QD/PVA and SiO₂-*h*-QD-MSMA/PMMA films, and the films after exposure to daylight for one year (SiO₂-*h*-QD/PVA1 and SiO₂-*h*-QD-MSMA/PMMA1). (b) UV-vis transmittance spectra of neat PVA and PMMA, newly prepared SiO₂-*h*-QD/PVA and SiO₂-*h*-QD-MSMA/PMMA, and the films after exposure to daylight for one year (SiO₂-*h*-QD/PVA1 and SiO₂-*h*-QD-MSMA/PMMA1). (c) Photographs of transparent SiO₂-*h*-QD/PVA film (top) under daylight and under UV light (365 nm) (middle), and SiO₂-*h*-QD-MSMA/PMMA (bottom) films under UV light. The SiO₂-*h*-QD/PVA and SiO₂-*h*-QD-MSMA/PMMA films contain 0.5 wt% of SiO₂-*h*-QDs and SiO₂-*h*-QD-MSMAs nanohybrids, respectively. (d) TEM image of SiO₂-*h*-QD-MSMA/PMMA, indicating the good dispersion of the SiO₂-*h*-QD-MSMAs nanohybrids in the PMMA matrix. The inset of (d) shows the high-resolution TEM image, confirming the existence of CdTe QDs.

films are quite stable and no obvious decrease of photoluminescence and transparency can be detected even under UV light for 24 h or under daylight over one year as shown in Fig. 2a,b. This good stability is very important for practical applications of composite films.

To probe whether the SiO₂-*h*-QDs are well dispersed in the polymer matrix, transmission electron microscopy (TEM) studies were performed. Fig. 2d shows a typical TEM image of the SiO₂-*h*-QD-MSMA/PMMA, and the SiO₂-*h*-QD-MSMAs nanohybrids are uniformly distributed in the PMMA matrix without obvious aggregation. The inset high-resolution TEM image shows that the CdTe QD crystal structure was well retained. Such a fine dispersing effect in turn explains the reason for the strong photoluminescence and high transparency of the films.

So robust QD-polymer composite films with strong and stable photoluminescence properties can be accessed readily, which lays the foundation for investigating the mechanical enhancing effect of QD fillers.

Generally, for polymer/silica nanocomposites, three main requirements are needed for silica to enhance the mechanical performance of composites: small size, good dispersion, and strong interfacial strength.^{22–25} Silica particles with large size (e.g., above 1 μm) may cause phase segregation between the interface of SiO₂ and polymer matrix, and thus the interfacial strength is not strong enough. The weak interface will break down first and the SiO₂ domains become the weak points in

composites, and further deteriorate the mechanical properties.²⁶ To describe the effect of large size silica fillers on composites, Nicolais *et al.*²⁷ proposed the following equation

$$\sigma_c = \sigma_m(1 - 1.21V_f^{2/3}) \quad (1)$$

where σ_c and σ_m are the tensile strength of the composite and neat polymer, respectively. V_f is the filler volume fraction, which can be calculated using the following equation:

$$V_f = \rho_m W_f / [(\rho_m - \rho_f)W_f + \rho_f] \quad (2)$$

where W_f is the weight fraction of filler, ρ_f and ρ_m are the density of filler (here for SiO₂-*h*-QDs or SiO₂-*h*-QD-MSMA: 2.5 g/cm³) and polymer matrix (for PMMA, 1.18 g/cm³), respectively. It can be seen that the strength of the composite cannot be greater than the strength of the corresponding polymer when the fillers are of large size. However, for ultrasmall silica fillers (below 30 nm), they tend to aggregate in the polymer matrix because of strong van der Waals forces. One of the effective ways to prevent the aggregation is to modify the silica surface with organic components.²⁶ Additionally, this modification can greatly improve the compatibility associated with interfacial strength between the nanofillers and matrices.^{28,29} Here, for our synthesized fluorescent SiO₂-*h*-QDs nanohybrids, they are ultrasmall and their surface can be easily modified to improve the SiO₂-*h*-QDs dispersion in polymers as well as enhance the interfacial strength between the SiO₂-*h*-QDs and polymer. Therefore, it is expected that the SiO₂-*h*-QD-polymer nanocomposites will exhibit enhanced mechanical properties.

The representative stress-strain curves of nanocomposites of PMMA reinforced with modified SiO₂-*h*-QD-MSMAs are shown in Fig. 3a. The tensile strength, Young's modulus, and elongation at break of the nanocomposites are given in Table 1. To our delight, both the tensile strength and Young's modulus of the nanocomposites are generally much higher than the corresponding neat polymer without compromising the elongation at break when the concentrations of SiO₂-*h*-QD-MSMAs are relatively low (<0.5 wt%). Particularly, for the SiO₂-*h*-QD-MSMA/PMMA film, the tensile strength, Young's modulus, and elongation at break improved by about 46%, 74% and 6% respectively, upon the loading of only 0.2 wt% of SiO₂-*h*-QD-MSMAs.

Theoretically, for the composite filled with ultrasmall silica, Sumita *et al.*³⁰ proposed an equation to describe enhanced effect of the nanofillers on composites as follows:

$$\tau_c = \tau_m(1 - V_f^{2/3}) + \frac{Gb}{k_{(d)} \left[\left(\frac{4\pi}{3V_f} \right)^{1/3} - 2 \right]} \cdot \frac{d}{2} \quad (3)$$

where τ_c (assuming $\tau_c = 1/2 \sigma_c$) and τ_m are the shear stress of the composite and neat polymer, respectively, G is the shear modulus, b is Burger's vector, d is the diameter of the filler (for our nanofillers: $d = 13$ nm), and $k_{(d)}$ is an aggregation parameter. By comparing the tensile strengths shown in Fig. 3a and Table 1, the values of $Gb/k_{(d)}$ were calculated as shown in Fig. 3b. Since Gb is constant for a given matrix PMMA, $k_{(d)}$ increases with the SiO₂-*h*-QD-MSMAs weight fraction when W_f is over the optimized value (0.2 wt%). Hence the addition of excess SiO₂-*h*-QD-MSMAs can cause aggregation, which may cause the decrease of

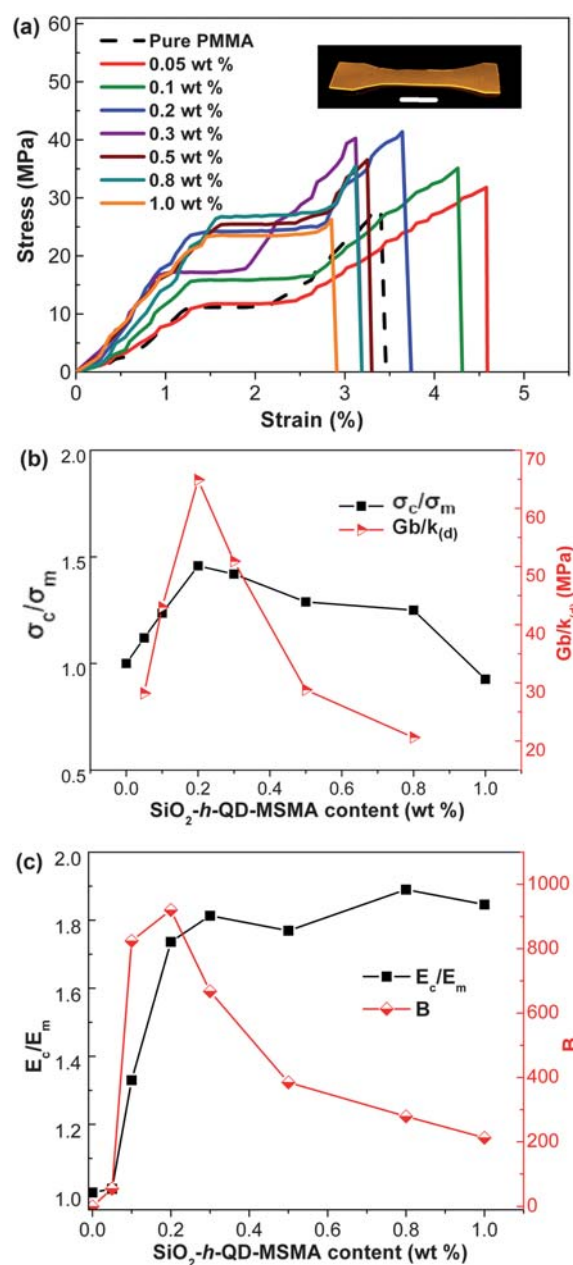


Fig. 3 (a) Representative stress-strain curves of pure PMMA and SiO₂-*h*-QD-MSMA/PMMA nanocomposites. (b) Values of $Gb/k_{(d)}$ of PMMA composites against the content of SiO₂-*h*-QD-MSMA. (c) Values of B of PMMA composites against the content of SiO₂-*h*-QD-MSMA. The inset of (a) is a representative SiO₂-*h*-QD-MSMA/PMMA dog-bone specimen for mechanical testing (the scale bar is 1 cm), and its SiO₂-*h*-QD-MSMA content is 0.5 wt%.

tensile strength and elongation at break.^{30–32} In fact, the addition of 1.0 wt% of SiO₂-*h*-QD-MSMAs caused the decrease of the tensile strength and elongation at break by 7% and 17%, respectively, which is in agreement with the calculated result. Therefore, to obtain high performance nanocomposites only very low contents of SiO₂-*h*-QD-MSMAs nanofillers (<1.0 wt%) are required.

On the other hand, the additions of SiO₂-*h*-QD-MSMAs can greatly increase the Young's modulus as well (Table 1). The main

Table 1 Mechanical properties of fluorescent SiO₂-*h*-QD-MSMA/polymer nanocomposites

SiO ₂ - <i>h</i> -QD-MSMAs content (wt%)	Tensile Strength (MPa)	Young's Modulus (GPa)	Elongation at Break (%)
PMMA blank	28.4 ± 1.2 (0%) ^a	0.91 ± 0.05 (0%)	3.42 ± 0.08 (0%)
PMMA-0.05	31.8 ± 0.8 (12%)	0.89 ± 0.04 (-2%)	4.63 ± 0.10 (35%)
PMMA-0.1	35.1 ± 1.3 (24%)	1.21 ± 0.06 (33%)	4.35 ± 0.08 (27%)
PMMA-0.2	41.4 ± 1.5 (46%)	1.58 ± 0.08 (74%)	3.62 ± 0.09 (6%)
PMMA-0.3	40.3 ± 1.0 (42%)	1.65 ± 0.09 (81%)	3.13 ± 0.11 (-8%)
PMMA-0.5	36.6 ± 0.7 (29%)	1.61 ± 0.07 (77%)	3.14 ± 0.08 (-8%)
PMMA-0.8	35.5 ± 0.8 (25%)	1.72 ± 0.04 (89%)	3.10 ± 0.07 (-10%)
PMMA-1.0	26.3 ± 0.6 (-7%)	1.68 ± 0.04 (85%)	2.85 ± 0.07 (-17%)
PS blank	29.3 ± 0.6 (0%)	2.21 ± 0.03 (0%)	1.92 ± 0.06 (0%)
PS-0.15	32.5 ± 0.6 (11%)	3.10 ± 0.05 (33%)	2.15 ± 0.07 (12%)
PS-0.25	32.8 ± 0.5 (12%)	3.75 ± 0.05 (47%)	2.36 ± 0.05 (23%)
PS-0.5	29.5 ± 0.5 (1%)	3.65 ± 0.04 (42%)	2.04 ± 0.05 (6%)
PS-1.0	30.6 ± 0.5 (5%)	4.01 ± 0.02 (94%)	1.93 ± 0.04 (1%)

^a Value in parentheses represents percentage increase/decrease as compared to the polymer.

reason is likely due to the strong interfacial force between nanofillers and polymer,^{33–35} which could be estimated according to the famous Einstein equation:^{35–37}

$$E_c = E_m(1 + BV_f) \quad (4)$$

where E_c and E_m are the Young's moduli of the composite and matrix, respectively, and B is a constant parameter related to the interface adhesion between filler and polymer matrix. If there is no adhesion between filler and matrix, $B = 1$, while for strong adhesion B takes values higher than 2.5. As can be seen from Fig. 3c, the constant B calculated from the Einstein equation for the SiO₂-*h*-QD-MSMA/PMMA nanocomposites is far higher than 2.5, suggesting that the adhesion between the SiO₂-*h*-QD-MSMAs and PMMA matrices is very strong. In addition, the comparable or even higher elongation at break of the SiO₂-*h*-QD-MSMA/PMMA nanocomposites as compared with the corresponding pure PMMA is also attributed to the strong adhesion strength besides the good dispersion of the SiO₂-*h*-QD-MSMAs nanofillers in PMMA matrices.

In the true applications, it is no doubt that a kind of general filler would be much more popular than a special one. To demonstrate the generality of the enhancing effect of the QD fillers, composite films of SiO₂-*h*-QD-MSMA and polystyrene (PS) were fabricated according to the same protocol as that of PMMA cases (Fig. 4 and Table 1). For SiO₂-*h*-QD-MSMA/PS films, the loading of 0.25 wt% of SiO₂-*h*-QD-MSMAs can also lead to improvements in tensile strength, Young's modulus, and elongation at break by about 12%, 47% and 23%, respectively.

For comparison, unmodified SiO₂-*h*-QDs and SiO₂-MSMAs with mean diameter 30 nm were also used to fabricate the PS composites using the same procedure as the SiO₂-*h*-QD-MSMAs, respectively (Fig. S3 and S4†). The results show that no obvious enhancement of tensile strength but a serious decrease of elongation at break of PS can be observed for the addition of unmodified SiO₂-*h*-QDs (Fig. S3†), due to the poor compatibility of polar surfaces of SiO₂-*h*-QDs and nonpolar PS matrix. For the addition of SiO₂-MSMAs, the slight increase results of tensile strength and elongation at break can be achieved at low content of SiO₂-MSMAs (e.g., 0.15 wt%), but great decreases of elongation at break of the PS composites were found for the relatively high load contents (e.g., 0.5 wt%) (Fig. S4†). All these results

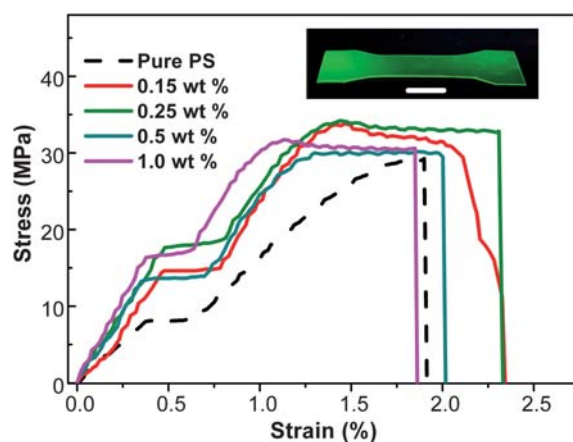


Fig. 4 Representative stress-strain curves of pure PS and SiO₂-*h*-QD-MSMA/PS nanocomposites. The inset is a representative SiO₂-*h*-QD-MSMA/PS dog-bone specimen for mechanical testing (the scale bar is 1 cm), and its SiO₂-*h*-QD-MSMA content is 0.5 wt%.

indicate that the mechanical enhancement of PS by the nanofillers of SiO₂-*h*-QD-MSMAs is much better than by the pristine SiO₂-*h*-QDs and SiO₂-MSMAs, because of their good dispersion in PS matrix, strong adhesion strength derived from the modified surface, and ultrasmall size.

In addition, the mechanical reinforcement of SiO₂-*h*-QD/PVA films was also observed as shown in Fig. S2† (e.g.; the tensile strength improved by 22% upon the addition of 0.25 wt% of SiO₂-*h*-QDs). Therefore, the SiO₂-*h*-QD is deserved as a kind of general and versatile nanofiller that not only endows stable photoluminescence properties to polymer films but also improves their mechanical properties.

To further study the mechanical enhancement behavior of the nanocomposites, scanning electron microscopy (SEM) images of the fracture surfaces of SiO₂-*h*-QD-MSMA/PS, neat PS, and PS filled with unmodified SiO₂-*h*-QDs were recorded as shown in Fig. 5. It could be seen that the neat PS exhibited a typical brittle behavior with smooth fracture surface, demonstrating that the neat PS is a typical brittle material (Fig. 5a,b). However, after the addition of SiO₂-*h*-QD-MSMAs, the fracture surface (Fig. 5c,d,e and f) became unsmooth with many pleats appeared. This

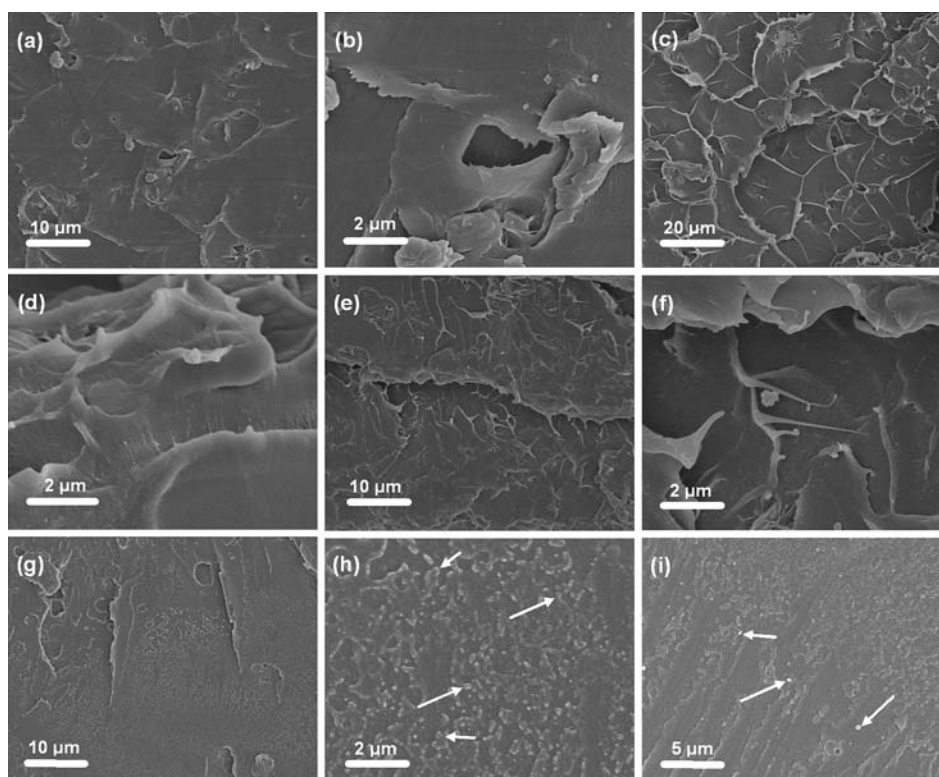


Fig. 5 Representative SEM images of pure PS (a, b), and SiO₂-h-QD-MSMA/PS nanocomposites filled with 0.25 wt% (c, d) and 0.5 wt% (e, f) of SiO₂-h-QD-MSMAs. SEM images of PS composites filled with 0.25 wt% (g, h) and 0.5 wt% (i) of unmodified SiO₂-h-QDs.

indicated that the nanocomposites presented a ductile rupture behavior, which is totally different fracture behavior from the neat PS. In addition, SiO₂-h-QD-MSMAs nano hybrids are not discernible on the fracture surfaces of the nanocomposites even at relative high content (0.5 wt %), confirming the absence of aggregated SiO₂-h-QD-MSMAs in the PS matrix (Fig. 5c,d,e and f). In contrast, for the sample filled with unmodified SiO₂-h-QDs, the SiO₂-h-QDs aggregates with sizes of 40–100 nm can be clearly observed on the relatively smooth fracture surface (Fig. 5g,h and i). Therefore, we can conclude that the surface modification can significantly improve the SiO₂-h-QDs dispersion and thus accompanied by excellent mechanical properties.

Conclusions

In conclusion, we demonstrated for the first time that QD-polymer nanocomposites with both stable fluorescence emission and enhanced mechanical properties can be easily obtained by simply blending the silica hybridized CdTe QDs with polymers. It is believable that such an exploration would open a new area for applications of QDs, and largely extend their use from potential bio-nanotechnology to common industries.

Acknowledgements

This work was financially supported by the National Natural Science Foundation of China (No. 50773038 and No. 20974093), National Basic Research Program of China (973 Program, No. 2007CB936000), Science Foundation of Chinese University, and

the Foundation for the Author of National Excellent Doctoral Dissertation of China (No. 200527).

References

- 1 N. Tomczak, D. Jańczewski, M. Y. Han and G. J. Vancso, *Prog. Polym. Sci.*, 2009, **34**, 393.
- 2 D. Ciprari, K. Jacob and R. Tannenbaum, *Macromolecules*, 2006, **39**, 6565.
- 3 Y. Y. Peng, T. E. Hsieh and C. H. Hsu, *Appl. Phys. Lett.*, 2006, **89**, 211909.
- 4 R. P. Raffaele, S. L. Castro, A. F. Hepp and S. G. Bailey, *Progr. Photovolt.: Res. Appl.*, 2002, **10**, 433.
- 5 I. Robel, V. Subramanian, M. Kuno and P. V. Kamat, *J. Am. Chem. Soc.*, 2006, **128**, 2385.
- 6 M. Wang, N. Felorzabihi, G. Guerin, J. C. Haley, G. D. Scholes and M. A. Winnik, *Macromolecules*, 2007, **40**, 6377.
- 7 H. Skaff, Y. Lin, R. Tangirala, K. Breitenkamp, A. Böker, T. P. Russell and T. Emrick, *Adv. Mater.*, 2005, **17**, 2082.
- 8 Y. Guo and M. G. Moffitt, *Macromolecules*, 2007, **40**, 5868.
- 9 S. Chen, J. Zhu, Y. Shen, C. Hu and L. Chen, *Langmuir*, 2007, **23**, 850.
- 10 M. D. Goodman, J. Xu, J. Wang and Z. Lin, *Chem. Mater.*, 2009, **21**, 934.
- 11 S. Y. Yang, Q. Li, L. Chen and S. Chen, *J. Mater. Chem.*, 2008, **18**, 5599.
- 12 H. X. Shen, L. Chen and S. Chen, *J. Inorg. Organomet. Polym. Mater.*, 2009, **19**, 374.
- 13 L. Zhou, C. Gao, X. Z. Hu and W. J. Xu, *ACS Appl. Mater. Interfaces*, 2010, **2**, 1211.
- 14 H. Skaff, M. F. Ilker, E. B. Coughlin and T. Emrick, *J. Am. Chem. Soc.*, 2002, **124**, 5729.
- 15 L. Zhou, C. Gao and W. J. Xu, *J. Mater. Chem.*, 2009, **19**, 5655.
- 16 L. Zhou, C. Gao, W. J. Xu, X. Wang and Y. H. Xu, *Biomacromolecules*, 2009, **10**, 1865.
- 17 Y. H. Yang and M. Y. Gao, *Adv. Mater.*, 2005, **17**, 2354–2357.

-
- 18 R. Koole, M. M. van Schooneveld, J. Hilhorst, C. M. Donegá, D. C. Hart, A. van Blaaderen, D. Vanmaekelbergh and A. Meijerink, *Chem. Mater.*, 2008, **20**, 2503.
 - 19 M. Darbandi, R. Thomann and T. Nann, *Chem. Mater.*, 2005, **17**, 5720.
 - 20 Y. H. Yang, L. H. Jing, X. L. Yu, D. D. Yan and M. Y. Gao, *Chem. Mater.*, 2007, **19**, 4123.
 - 21 C. W. Lai, Y. H. Wang, Y. C. Chen, C. C. Hsieh, B. P. Uttam, J. K. Hsiao, C. C. Hsu and P. T. Chou, *J. Mater. Chem.*, 2009, **19**, 8314.
 - 22 J. H. Chen, M. Z. Rong, W. H. Ruan and M. Q. Zhang, *Compos. Sci. Technol.*, 2009, **69**, 252.
 - 23 M. Fujiwara, K. Kojima, Y. Tanaka and R. Nomura, *J. Mater. Chem.*, 2004, **14**, 1195.
 - 24 F. Yang and G. L. Nelson, *J. Appl. Polym. Sci.*, 2004, **91**, 3844.
 - 25 E. Kontou and G. Anthoulis, *J. Appl. Polym. Sci.*, 2007, **105**, 1723.
 - 26 H. Mahfuz, M. Hasan, V. Dhanak, G. Beamson, J. Stewart, V. Rangari, X. Wei, V. Khabashesku and S. Jeelani, *Nanotechnology*, 2008, **19**, 445702.
 - 27 L. Nicolais and M. Narkis, *Polym. Eng. Sci.*, 1971, **11**, 194.
 - 28 C. L. Wu, M. Q. Zhang, M. Z. Rong and K. Friedrich, *Compos. Sci. Technol.*, 2005, **65**, 635.
 - 29 G. Ragosta, M. Abbate, P. Musto, G. Scarinzi and L. Mascia, *Polymer*, 2005, **46**, 10506.
 - 30 M. Sumita, Y. Tsukumo, K. Miyasaka and K. Ishikawa, *J. Mater. Sci.*, 1983, **18**, 1758.
 - 31 W. H. Ruan, M. Q. Zhang, M. Z. Rong and K. Friedrich, *J. Mater. Sci.*, 2004, **39**, 3475.
 - 32 A. P. Kumar, D. Depan, N. S. Tomer and R. P. Singh, *Prog. Polym. Sci.*, 2009, **34**, 479.
 - 33 K. Sahakaro and S. Beraheng, *J. Appl. Polym. Sci.*, 2008, **109**, 3839.
 - 34 R. Y. Hong, H. P. Fu, Y. J. Zhang, L. Liu, J. Wang, H. Z. Li and Y. Zheng, *J. Appl. Polym. Sci.*, 2007, **105**, 2176.
 - 35 D. N. Bikiaris, A. Vassiliou, E. Pavlidou and G. P. Karayannidis, *Eur. Polym. J.*, 2005, **41**, 1965.
 - 36 A. Einstein, *Ann. Der. Phys.*, 1906, **324**, 289.
 - 37 J. Oberdisse, *Macromolecules*, 2002, **35**, 9441.